NANO LETTERS

2007
Vol. 7, No. 3
785−790

Rhodium Nanoparticles from Cluster Seeds: Control of Size and Shape by Precursor Addition Rate

Simon M. Humphrey, Michael E. Grass, Susan E. Habas, Krisztian Niesz, Gabor A. Somorjai,* and T. Don Tilley*

Department of Chemistry, University of California, Berkeley, California 94720, and the Chemical and Materials Sciences Divisions, Lawrence Berkeley National Laboratory, 1 Cyclotron Road, Berkeley, California 94720

Received January 5, 2007; Revised Manuscript Received January 28, 2007

ABSTRACT

The size-tunable synthesis of poly(vinylpyrrolidone)-stabilized cuboctahedral rhodium nanoparticles with mean diameters ranging between 3–7 nm and multipod structures was accomplished using seeded growth methods. Isotropic PVP-capped 2.9 nm seeds were prepared by ligand exchange on rhodium-triphenylphosphine metal–organic clusters. Quantitative investigation of reaction parameters in ethylene glycol revealed that size and shape could be controlled at a single reaction temperature of 120 °C. The rate of rhodium monomer addition was found to be critical for monodispersity and shape control, regardless of thermodynamic factors. Solvent viscosity, varied by changing the polyol solvents, indicated that autocatalytic addition kinetics are responsible for isotropic versus anisotropic growth.

Precise control of the size and shape of nanoparticles formed by solution-phase synthesis is currently a major goal in nanoscience.[1] Size and shape are physical attributes of critical importance because they directly influence solid-state phenomena that are unique to the nanoscale. Catalytic,[2] magnetic,[3] and optical[4] properties, for example, can in principle be tailored with synthetic design. For optimization of catalytic properties,[2,5] correlations must be established between nanoparticle structure and catalytic performance. The establishment of such principles requires reliable synthetic routes to nanoparticles of predetermined size and shape. Currently, a few synthetic methodologies exist for size- and shape-selected semiconductor[1a,6] and metal oxide[7] nanocrystals. Progress has also been made in the synthesis of well-defined noble metal nanocrystals, and this topic is of great interest given the importance of such particles in catalysis.[2,5] Rhodium nanoparticles are particularly important as catalytic species, and several reports have described the synthesis of well-defined nanocrystals of this type.[8,9] Finke and co-workers have prepared rhodium nanoparticles with a narrow size distribution, stabilized by polyoxoanions and tetrabutylammonium cations.[10] However, detailed investigations of structure−property relationships for supported Rh nanoparticles requires new synthetic methods that offer improved control of shape over a wide range of particle sizes.

The seeded growth method for nanoparticle synthesis is a promising two-step approach that separates thermodynamically disfavored nucleation processes from subsequent growth steps that occur spontaneously via addition of monomers to existing nanoparticles.[11] This strategy has recently been demonstrated for several metals, including Rh[8] and Pt.[12] Seed particles may be generated by fast solution-phase reduction of a metal precursor at elevated temperature in the presence of stabilizing agents. Seeds may then be isolated, purified, and functionalized as required. Growth occurs by addition of further metal atoms to the seeds under conditions that disfavor concomitant nucleation of new particles. This method potentially offers synthetic control that is not easily achieved from other methods.

The ideal seeds for growth of uniform particles are nucleates that are perfectly monodisperse. Over the past half century, several crystalline rhodium−organic cluster compounds with precise compositions have been reported such as Rh carbonyls and nitridocarbonyls.[13] These species contain very small metal clusters of 4−30 atoms, whose stability is gained from strongly bound organic ligands that bridge adjacent surface metal atoms. Clusters comprised of only a few metal atoms are likely to be unstable in solution as naked seeds, and the lattice structures of their "cores" may differ from those required for stable nanoparticles. In the 1980s, Schmid and co-workers reported a series of stable, cuboctahedral metal clusters that appeared to contain a magic number of metal atoms. These clusters, of Ru, Rh, Pt, and

* Corresponding authors. E-mail: somorjai@berkeley.edu (G.A.S.); tdtilley@berkeley.edu (T.D.T.).

10.1021/nl070035y CCC: $37.00
Published on Web 02/09/2007

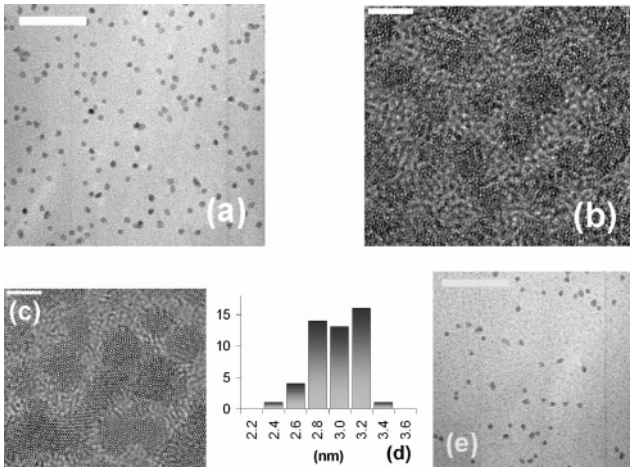

Figure 1. (a) TEM image of Rh−PPh_3 clusters (bar = 45 nm); (b) initial HRTEM image showing lack of crystallinity (bar = 3.0 nm); (c) particles after >30 min exposure to electron beam; (d) size distribution histogram obtained from HRTEM images of Rh−PPh_3; (e) TEM image of ligand-exchanged Rh−PVP particles (bar = 45 nm).

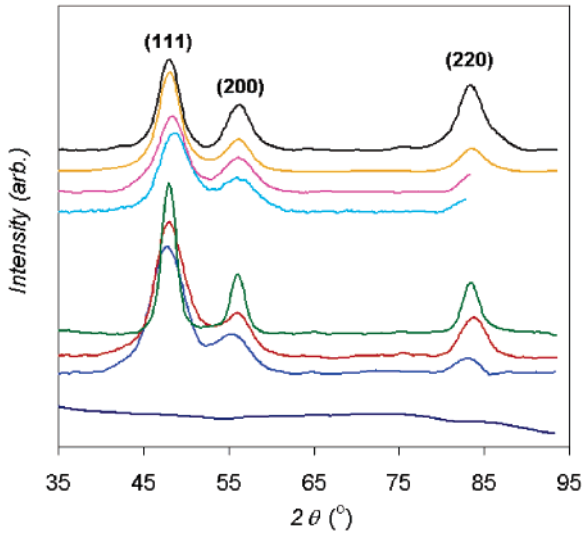

Figure 2. XRD data for Rh particles obtained by seeded growth: in ascending order, Rh−PVP 2.9 nm seeds showing no bulk diffraction (navy); 4.87 nm (blue) and 6.64 nm (red) cuboctahedra; 11.48 nm blocks (green); multipods prepared with 20.3 mg (cyan), 31.8 mg (magenta), 40.0 mg (yellow), and 50.4 mg $RhCl_3$ (black).

Au, are stabilized by chloride and phosphine ligands.[14,15] In this contribution, we report a similar method for production of Rh seed particles, which were found to be suitable precursors for growth of larger monodisperse Rh nanoparticles.

To prepare the seeds, a stirred solution of freshly prepared Wilkinson's catalyst, $(Ph_3P)_3RhCl$, in THF or benzene,[16] was partially reduced at 60 °C over 45 min by a stream of excess B_2H_6 that was generated in situ by the addition of BF_3-etherate to a slurry of $NaBH_4$/DME. After removal of solvent, the brown oily residue was washed with benzene and petroleum ether under N_2 to remove $Ph_3P{-}BH_nCl_{3-n}$ adducts, resulting in a dark-brown powder. Treatment of the powder with benzene should be minimized because prolonged washing results in significant dissolution. Note: Careful manipulation of the material under N_2 or Ar and in rigorously dried solvents is essential because the dried brown product is highly pyrophoric and readily ignites in air. Experiments attempted using either THF or benzene as the solvent resulted in material with nearly identical compositions, as determined by elemental analysis.[17] A single sharp resonance was consistently observed in the ^{31}P NMR spectrum, suggesting lability of the PPh_3 stabilizing groups on the surface of the Rh clusters. Analysis by transmission electron microscopy (TEM) and high-resolution TEM (HRTEM),[18] as shown in Figure 1, revealed that the $Rh_{\sim 500}/PPh_3$ clusters were highly monodisperse 2.9 nm spheres with $\sigma = 0.2$ nm (measured by pixel counting of 50 particles from HRTEM images to give a calculated range of $Rh_{430-645}$ based on ideal cuboctahedra). The cluster size was consistent between various synthetic runs. Clusters of this size contain approximately 500 Rh atoms, assuming a cuboctahedral shape. Rh and P elemental analyses are consistent with an approximate 1:1 ratio of PPh_3 to surface Rh atoms, calculated assuming 2.9 nm cuboctahedra clusters with a 1:1 ratio of (100):(111) faces. Hence, it is likely that a significant portion of the PPh_3 ligands are not directly bound to Rh surface atoms, especially given the steric requirements of the phosphines. HRTEM images indicate that the particles are polycrystalline, as they exhibit multiple crystalline domains (Figure 1c). Contrast and atomic ordering were both found to improve significantly with longer electron beam exposure time, presumably as organic material was removed and the particles were annealed. In support of these observations, a freshly prepared sample of $Rh_{\sim 500}/PPh_3$ exhibited no bulk diffraction between 30 and 100° 2θ by X-ray powder diffraction analysis (XRD).

The Rh clusters have low solubility in most organic solvents, but are soluble in CH_2Cl_2 and coordinating solvents such as pyridine and THF. Decomposition is rapid in wet solvents and occurs within hours in dry coordinating solvents. Therefore, attempts were made to exchange the capping agent[19] with the polymeric stabilizer poly(vinylpyrrolidone) (PVP) to stabilize the clusters and make them more soluble. The $Rh_{\sim 500}/PPh_3$ clusters and excess PVP (55 000 M_w) were stirred in THF/CH_2Cl_2 (1:1) at room temperature.[20] The PVP-capped Rh particles were initially precipitated with wet hexane and collected by centrifugation (4.2 krpm, 5 min). Several, further precipitations from ethanol with hexane removed any residual PVP and PPh_3. The resulting product is stable in aqueous or alcoholic solution for months. TEM and HRTEM analysis of the $Rh_{\sim 500}$/PVP material showed that the mean cluster size was not altered by the ligand exchange procedure (Figure 1e).[19] The $Rh_{\sim 500}$/PVP particles exhibited no diffraction by XRD, indicating polycrystallinity as observed for the precursor seeds (Figure 2). Elemental analysis of the purified Rh−PVP material confirmed almost complete removal of PPh_3 ($P = 0.34\%$), while 9.0% N corresponds to approximately 7 PVP monomer units per Rh surface atom. Thus, a large amount of polymer was incorporated despite the limited number of monomer units that can bind to the cluster via C═O···Rh or N···Rh donor interactions. A strong, broad C═O stretch and less intense C−H modes of the polymer were observed in the solid-state FTIR spectrum of $Rh_{\sim 500}$/PVP, and these bands were not

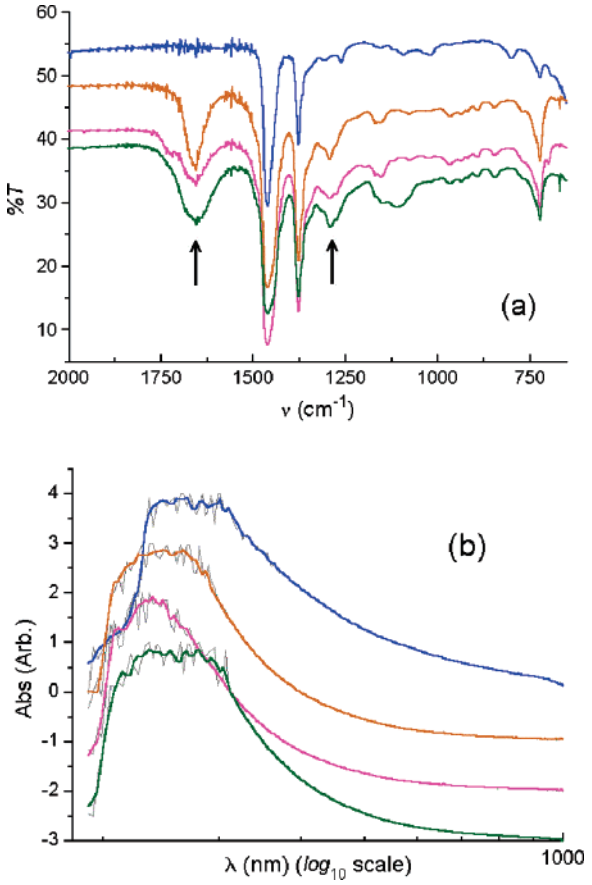

Figure 3. (a) FT−IR spectra (nujol mull) and (b) UV−vis spectra (in ethanol): Rh−PPh_3 (blue); Rh−PVP directly after ligand exchange (orange); Rh−PVP after first purification (magenta), and after second purification (green).

diminished after two reprecipitation/centrifugation cycles (Figure 3a). The UV−vis spectrum of the $Rh_{\sim 500}$/PVP material revealed a blue-shift in the plasmon absorbance maximum relative to the PPh_3-capped precursor (∼40 nm, Figure 3b).

Under optimized reaction conditions, the crystalline $Rh_{\sim 500}$/PVP seeds in ethylene glycol were effectively used to grow larger, monodisperse cuboctahedral Rh particles with excellent reproducibility. The $Rh_{\sim 500}$/PVP clusters and a large excess of PVP were rapidly stirred in ethylene glycol at 120 ± 2 °C as $RhCl_3$ in ethylene glycol was added at a rate of 40 mg h^{-1} via syringe pump.[21] The growth was quantified by varying the total amount of $RhCl_3$ added in separate reactions and then measuring average particle sizes (by pixel counting of 200 particles from TEM images), examples of which are given in Figure 4. This data was then compared to the curve for average theoretical particle size versus amount of $RhCl_3$ added, which was calculated by assuming complete consumption of the precursor in layer-by-layer growth of Rh cuboctahedra (Figure 5, red line). Under optimized synthetic conditions, particle size could be accurately controlled in the range of 3−7 nm (Figure 5, blue squares). Near-monodisperse Rh nanoparticles were obtained with small standard deviations (Figure 4). Figure 4c exhibits the HRTEM image of a representative Rh particle (5.7 nm) with regular cuboctahedral shape, which was obtained by

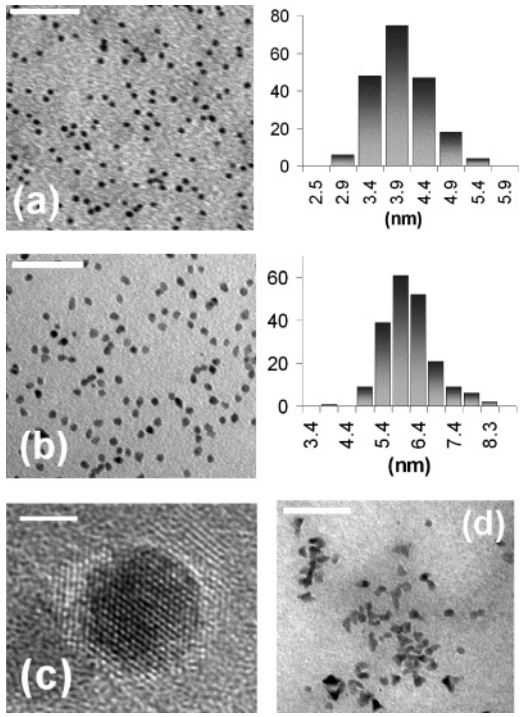

Figure 4. Examples of (a) 4.0 nm σ = 0.52 nm, (b) 6.11 σ = 0.70 nm (bar = 50 nm) Rh cuboctahedra shown with corresponding size histograms; (c) HRTEM of 5.65 nm cuboctahedron with FFT image inset (bar = 2.0 nm) (d) Rh particles prepared by direct addition of 20 mg $RhCl_3$ into ethylene glycol−PVP at 120 °C (no seeds).

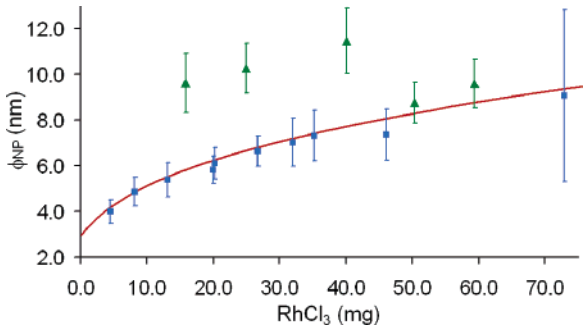

Figure 5. Graph of size control study of Rh cuboctahedra growth (blue squares with standard deviation bars) vs calculated size (red line). Particle sizes obtained from slow addition rate syntheses (10 mg h^{-1}) are shown plotted as green triangles with standard deviation bars.

the seeded growth method. The average spacing between atomic planes (d = 0.21 nm) and the hexagonal symmetry of atomic ordering corresponds to an Rh(111) surface. HRTEM confirmed the crystallinity of the particles, a small portion of which contained visible grain boundaries. XRD studies confirmed bulk crystallinity (Figure 2). To confirm that seeded growth was responsible for the formation of Rh cuboctahedra, $RhCl_3$ was added to ethylene glycol and PVP at 120 °C in the absence of seeds. These conditions resulted in reduction of $RhCl_3$ and the formation of 2−10 nm particles with variable, poorly defined shapes (Figure 4d).

Attempts to directly grow particles >7 nm in size consistently resulted in particle samples with large size distributions and shape anisotropies. It is not readily apparent

why larger particles are not accessible via this route. The growth of larger particles may be slowed as the particle surface becomes more stable via deactivation of larger faces by the PVP capping agent. However, larger particles were found to form upon extended heating, presumably via Ostwald ripening; heating monodisperse 6 nm Rh particles for 8 h (at 120 °C) in the presence of excess PVP led to a mixture of 6−20 nm globular-shaped particles.

It seemed that the observed size limitation for this synthetic method might be associated with factors that determine the diffusion rate of monomer units to the growing particle. This was investigated by changing the synthetic conditions, via variations in the initial concentration of rhodium, and in the rate of addition of rhodium to the reaction mixture. First, the total solvent volume was varied between 5 and 20 cm^3, with 10−50 mg of $RhCl_3$ added to the $Rh_{\sim 500}$/PVP seeds. All other factors including stirring rate were unchanged. Interestingly, more or less concentrated solutions (compared to the original, optimized concentration for growth[21]) gave higher polydispersities and poorer synthetic control. Second, it was found that variations in the rate of $RhCl_3$ addition, between 10 and 160 mg h^{-1}, allowed an unexpectedly high level of shape control for the resulting particles. Slow monomer addition (10 mg h^{-1}) formed 9−11.5 nm block-shaped particles (Figure 6). These sizes are also plotted in Figure 5 (triangles), which illustrates how the resulting particle dimensions are approximately constant for addition of 15−60 mg of $RhCl_3$ to 1.25 mg of $Rh_{\sim 500}$/PVP seeds. Thus, for growth reactions that occurred over long periods of time at 120 °C, Ostwald ripening was dominant, affording particles that are larger in size but fewer in number.

In contrast, when $RhCl_3$ was added rapidly at 160 mg h^{-1}, multipod structures were formed by highly anisotropic growth. TEM images confirmed that approximately 90% of the particles were branched in three or four directions (tripods and tetrapods), while others were V-shaped or spherical (unbranched). A representative HRTEM image of a tetrapod is shown in Figure 6g. Multipods appeared to be crystalline with lattice spacings on the arms indicative of (111) faces (d = 0.215 nm), as has been previously reported.[8,9] The observation of broad peaks corresponding to Rh (111), (200), and (220) reflections in the XRD spectrum confirmed bulk crystallinity (Figure 6). It is noteworthy that the average ratio of intensities of (111):(200) reflections for multipods was found to be 1.9, compared to 2.8 for cuboctahedral particles (see Supporting Information). This disparity is due to variations in X-ray coherence lengths for different crystal morphologies.[8] The average multipod arm length may be controlled by changing the amount of added precursor, as predicted by the seeded growth mechanism. Reduction of 20 mg of $RhCl_3$ with 1.25 mg of seeds formed pointed/tetrahedral intermediates, suggesting that growth occurred most rapidly at (111) faces from the onset of addition. Addition of 30, 40, or 50 mg of $RhCl_3$ increased the average arm lengths to approximately 7.1, 9.2, and 11.5 nm, respectively, while arm width remained constant (∼2.5 nm), as shown in Figure 6. Multipods with longer arms were also prepared by further precursor addition, but samples became increasingly less uniform with respect to the crystalline morphology.

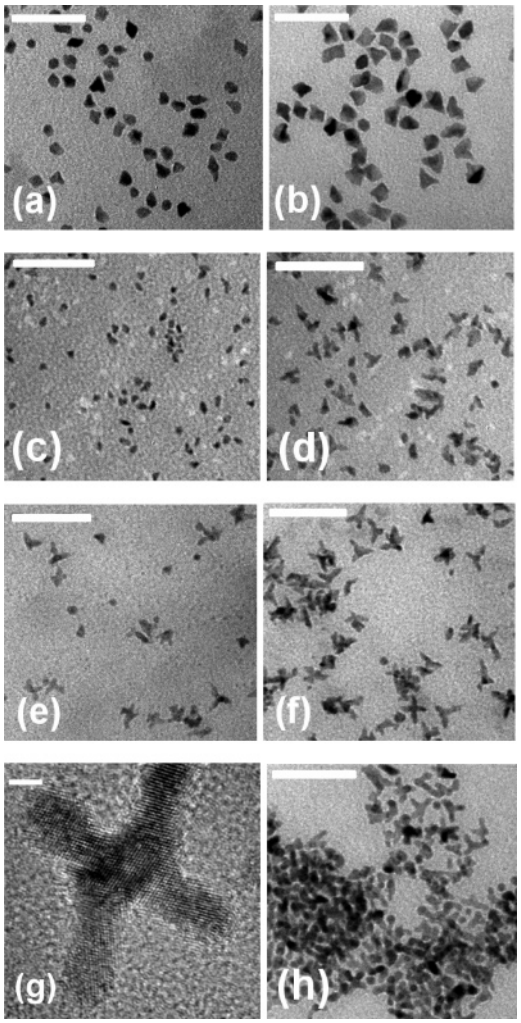

Figure 6. Particles obtained from slow (10 mg h^{-1}) addition of monomer for (a) 15.8 mg and (b) 40.1 mg $RhCl_3$. Rh multipods from rapid (160 mg h^{-1}) $RhCl_3$ addition: (c) 20.2 mg; (d) 31.8 mg; (e) 40.0 mg; (f) 50.4 mg (bar = 50 nm); (g) HRTEM image of tetrapod viewed with (111) arms (bar = 2.0 nm); (h) multipods after 24 h heating at 120 °C in ethylene glycol.

The above observations conform to a general model of growth, whereby slow monomer addition rates favor epitaxial growth onto all crystal faces, resulting in minimization of overall particle surface energy.[22] Rh cuboctahedra become branched via accelerated addition in the ⟨111⟩ direction when monomer is added at a rate that maintains excess Rh monomers in solution (the addition rate is faster than the consumption of precursor). Because multipods are not thermodynamically favored, their formation may be driven by kinetics governing relative addition at {111} versus {100} faces. Alternatively, arm growth can be explained by a mechanism of oriented attachment, whereby supersaturation of monomer in solution results in the formation of new nucleates that subsequently aggregate in an ordered fashion.[23] Xia and co-workers recently reported synthesis of Rh multipods with flower-petal-shaped arms by rapid reduction of anhydrous Na_3RhCl_6 in ethylene glycol/PVP at 140 °C.[9] They observed multipod formation within 5 min via a process

suggested to occur by rapid nucleation and anisotropic addition of residual monomers. Continued heating at 140 °C caused slow etching of the arms to form spherical particles after 2 days. When we performed this experiment with multipods prepared by addition of 50 mg of $RhCl_3$ to Rh−PVP seeds, only partial etching of arms was observed after 24 h at 120 °C, indicating kinetic stability at this temperature (Figure 6h). Moreover, multipods are not precursors to the cuboctahedra, and larger cubic particles are formed by an independent, thermodynamically controlled process over longer reaction times.

The influence of monomer addition rate on shape control is very similar to that observed previously for semiconductor nanocrystals.[6] However, in previously reported growth studies with Rh, shape control was observed to be directly associated with reaction temperature.[8] When concentrated $RhCl_3$ solution was added over 10 min to seeds prepared by in situ nucleation in ethylene glycol, irregular multipods with two to seven arms formed at 90 °C, while (100) cubes were obtained by an analogous procedure at 190 °C. Cubes with hornlike projections were also formed at intermediate temperatures, apparently due to competition between both modes of growth.[8] Because the investigation described here has identified conditions for the selective synthesis of multipods, cuboctahedra, and cubelike particles at a single reaction temperature, it was of interest to examine additional experimental parameters that might influence particle morphology. Diffusion, stirring rate, and solvent viscosity are interdependent synthetic variables that influence the frequency of monomer−particle collisions in solution.

A series of experiments were undertaken to study the effect of solvent viscosity on particle growth. At 90 °C the dynamic viscosity of ethylene glycol is 2.44 cP versus 0.64 cP at 190 °C ($\eta = 1.00$ cP for H_2O at STP) (see Supporting Information). To test the effect of a 4-fold change in viscosity on particle shape, solvents of different viscosities were employed at constant temperature. This was accomplished using the chemically similar 1,2-substituted polyols 1,2-propanediol ($C_3H_8O_2$) and 1,2-butanediol ($C_4H_{10}O_2$), which have $\eta = 2.03$ and 0.62 cP values, respectively, at 120 °C (cf. ethylene glycol, $\eta = 1.40$ at 120 °C). For both solvent systems, $RhCl_3$ was added to the $Rh_{\sim 500}$/PVP seeds at a rate of 10, 40, or 160 mg h^{-1} using otherwise identical conditions to those employed previously. For reactions in 1,2-propanediol, slow monomer addition gave polydisperse particles with sizes of 5−15 nm; an intermediate addition rate resulted in a mixture of elongated spheres and multipods, and poorly formed multipods were obtained from rapid addition (Figure 7a−c). The intermediate addition rate (40 mg h^{-1}) in ethylene glycol reproducibly afforded mondisperse cuboctahedra; therefore, the formation of mainly branched particles from more viscous solvent indicates a distinct change in the growth kinetics. In contrast, for all addition rates, growth in the less-viscous 1,2-butanediol resulted in unusual jigsaw-piece-shaped particles that are multiply branched (Figure 7d). These results indicate that viscosity may be a very important shape-directing variable. However, the small chemical differences in the solvents employed (due to the differing alkyl chains) and differing degrees of solvation of other ligands present (e.g., Cl^-) may also play a role.

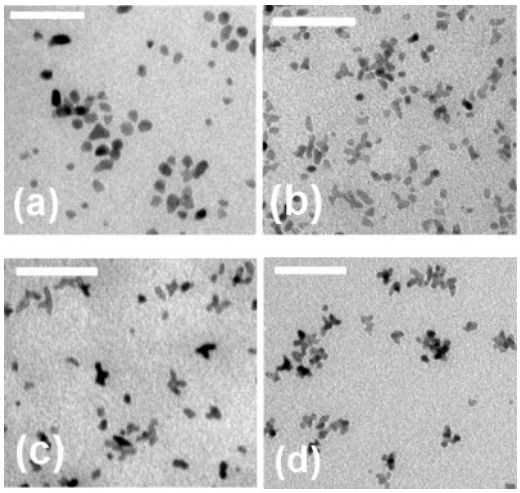

Figure 7. Rh nanoparticles prepared by addition of $RhCl_3$ to Rh−PVP seeds in 1,2-propanediol at (a) 10 mg h^{-1}; (b) 40 mg h^{-1}; (c) 160 mg h^{-1}; (d) jigsaw piece-shaped particles obtained for all monomer addition rates in 1,2-butanediol (bar = 50 nm).

In conclusion, improved size and shape selectivity has been demonstrated for Rh nanoparticles via control of the monomer addition rate. The formation of Rh cuboctahedra and multipod nanocrystals was reproducibly achieved by growth from isotropic Rh seed clusters under specific and controlled reaction conditions. Particle shape is not directly dependent on reaction temperature; however, the type of polyol solvent employed and the intrinsic solvent viscosity were demonstrated to be highly influential factors. Seeded growth, using the method described herein, may be used to prepare efficiently near-monodisperse Rh nanoparticles with varied shapes. We are presently studying the relationship between the size of supported Rh nanoparticle catalysts and product selectivity for a variety of reactions.

Acknowledgment. This work was supported by the Director, Office of Science, Office of Advanced Scientific Computing Research, Office of Basic Energy Sciences, Chemical Sciences, Geosciences, and Biosciences Division of the U.S. Department of Energy under contract no. DE-AC02-05CH11231. We thank the Berkeley Electron Microscopy Lab and the National Center for Electron Microscopy for access to TEM and HRTEM facilities. We also thank Prof. A. Paul Alivisatos for use of the powder diffractometer.

Supporting Information Available: Powder XRD (111):(200) intensity ratio data for Rh multipods, cuboctahedra, and larger particles. Size distribution histograms for data given in Figure 5. Plot of temperature versus dynamic viscosity of the polyols. This material is available free of charge via the Internet at http://pubs.acs.org.

References

(1) See, for example: (a) Yin, Y.; Alivisatos, A. P. *Nature* **2005**, *437*, 664; (b) Jun, Y.; Lee, J.-H.; Choi, J.; Cheon, J. *J. Phys Chem. B* **2005**, *109*, 14795; (c) Wang, X.; Zhuang, J.; Peng Q.; Li, Y. *Nature* **2005**, *437*, 121.

(2) (a) Roucoux, A.; Schultz, J.; Patin, H. *Chem. Rev.* **2002**, *102*, 3757; (b) Yu, W. W.; Liu, H. *J. Mol. Catal. A* **2006**, *243*, 120; (c) Johnson, B. F. G. *Coord. Chem. Rev.* **1999**, *190*, 1269; (d) Pohl, M.; Lyon, D. K.; Mizuno, N.; Nomiya, K.; Finke, R. G. *Inorg. Chem.* **1995**, *34*, 1413.
(3) (a) Magnani M.; Galluzzi L.; Bruce I. J. *J. Nanosci. Nanotechnol.* **2006**, *6*, 2302; (b) Morneta, S.; Vasseura, S.; Grassteb, F.; Veverkac, P.; Goglioa, G.; Demourguesa, A.; Portiera, J.; Pollertc E.; Duguet, E. *Prog. Solid State Chem.* **2006**, *34*, 237; (c) Huber, D. L. *Small* **2005**, *1*, 482.
(4) Alivisatos, A. P. *Science* **1996**, *271*, 933.
(5) See, for example: (a) Astruc, D.; Lu, F.; Aranzaes, J. R. *Angew. Chem., Int. Ed.* **2006**, *44*, 7852; (b) Narayanan, R.; El-Sayed, M. *A. J. Phys. Chem. B* **2005**, *109*, 12663.
(6) (a) Manna, L.; Scher, E. C.; Alivisatos, A. P. *J. Am. Chem. Soc.* **2000**, *122*, 12700; (b) Chu, H.; Li, X.; Chen, G.; Zhou, W.; Zhang, Y.; Jin, Z.; Xu, J.; Li, Y. *Cryst. Growth Des.* **2005**, *5*, 1801.
(7) Epifani, M.; Diaz, R.; Arbiol, J.; Comini, E.; Sergent, N.; Pagnier, T.; Siciliano, P.; Taglia, G.; Morante, J. R. *Adv. Funct. Mater.* **2006**, *16*, 1488 and references therein.
(8) Hofelmeyer, J. D.; Niesz, K.; Somorjai, G. A.; Tilley, T. D. *Nano Lett.* **2005**, *5*, 435.
(9) (a) Zettsu, N.; McLellan, J. M.; Wiley, B.; Yin, Y.; Li, Z.-Y.; Xia, Y. **2006**, *45*, 1288; (b) Marín-Almazo, M.; Ascencio, J. A.; Pérez-Álvarez, M.; Gutiérrez-Wing, C.; José-Yacamán, M. *Microchem. J.* **2005**, *81*, 133; (c) Harada, M.; Abe, D.; Kimura, Y. *J. Colloid Interface Sci.* **2005**, *292*, 113.
(10) (a) Widegren, J. A.; Finke, R. G. *Inorg. Chem.* **2002**, *41*, 1558; (b) Hornstein, B. J.; Aiken, J. D., III; Finke, R. G. *Inorg. Chem.* **2002**, *41*, 1625.
(11) Yu, H.; Gibbons, P. C.; Kelton, K. F.; Buhro, W. E. *J. Am. Chem. Soc.* **2001**, *123*, 9198.
(12) Niesz, K.; Grass, M. E.; Somorjai, G. A. *Nano Lett.* **2005**, *5*, 2238.
(13) See, for example: (a) Moszner, M.; Ziółkowski, J. J. *J. Organomet. Chem.* **1991**, *411*, 281; (b) Ciani, G.; Magni, A.; Sironi, A. *J. Chem. Soc., Chem. Commun.* **1981**, 1280; (c) Fumagalli, A.; Martinengo, S.; Bernasconi, Ciani, G.; Prosperio, D. M.; Sironi, A. *J. Am. Chem. Soc.* **1997**, *119*, 1450.
(14) Schmid, G. *Polyhedron* **1988**, *7*, 2321.
(15) Schmid, G.; Huster, W. *Z. Naturforsch.* **1986**, *41b*, 1028.
(16) We thank Prof. Schmid for this suggested alternative method via personal correspondence.
(17) Characterization data for Rh−PPh_3: ^{31}P NMR (C_5D_5N): $\delta = 27.2$ ppm, sharp singlet; C, 39.8; H, 3.72; Cl, 2.73; P, 5.85; Rh, 47.9 %.
(18) Samples of Rh−PPh_3 for TEM and HRTEM were prepared by evaporation of solvent from the support grid under an inert atmosphere. Clusters were subsequently exposed to air, so presumably the as-imaged species are oxidized at the surface.
(19) (a) Guo, R.; Song, Y.; Wang, G.; Murray, R. W. *J. Am. Chem. Soc.* **2005**, *127*, 2752; (b) Bagaria, H. G.; Ada, E. T.; Shamasuzzoha, M.; Nikles, D. E.; Johnson, D. T. *Langmuir* **2006**, *22*, 7732; (c) Woehrle G. H.; Hutchison, J. E. *Inorg. Chem.* **2005**, *44*, 6149; (d) Woehrle, G. H.; Brown, L. O.; Hutchison, J. E. *J. Am. Chem. Soc.* **2005**, *127*, 2172; (e) Petroski, J. C.; Mei, H.; Creutz, C. *Inorg. Chem.* **2004**, *43*, 1597.
(20) In a typical synthesis, 10 mg clusters and 25 mg PVP (55 000 M_w) were stirred in THF/CH_2Cl_2 (1:1, 40 cm^3) at room temperature over 2 h. The clusters were then precipitated by addition of bench hexane, collected by ultracentrifugation, and redispersed into ethanol with short cycles of sonication treatment (2 min). This procedure was repeated to ensure removal of excess PVP.
(21) Optimized conditions for growth: Rh−PVP (0.60 mg Rh) and 25 mg PVP in ethylene glycol (10.0 cm^3) at 120 ± 2 °C were rapidly stirred for 5 min. A solution of $RhCl_3$ in ethylene glycol (5.0 cm^3) was then injected directly into the solvent by cannula needle at a desired rate, controlled using syringe pump apparatus. Upon completion of addition, the deep-brown mixture was cooled to room temperature by quenching in a cold water bath. Precipitation was achieved with hexane/2-propanol, and the solid was redispersed into ethanol.
(22) Jiang, Q.; Lu, H. M.; Zhao, M. *J. Phys. Condens. Matter* **2004**, *16*, 521.
(23) (a) Banfield, J. F.; Welch, S. A.; Zhang, H.; Ebert, T. T.; Penn, R. L. *Science* **2000**, *289*, 751; (b) Rubeiro, C.; Lee, E. J. H.; Longo, E.; Leite, E. R. *ChemPhysChem.* **2005**, *6*, 690; (c) Drews, T. D.; Katsoulakis, M. A.; Tsapatsis, M. *J. Phys. Chem. B* **2005**, *109*, 23879.

NL070035Y